Multivariate pattern analysis of the neural correlates of smoking cue attentional bias

Amanda Elton[a,b], Vicki W. Chanon[a], Charlotte A. Boettiger[a,b,c,*]

[a] Department of Psychology and Neuroscience, University of North Carolina, Chapel Hill, NC, 27599, USA
[b] Bowles Center for Alcohol Studies, University of North Carolina, Chapel Hill, NC 27599, USA
[c] Biomedical Research Imaging Center, University of North Carolina, Chapel Hill, NC 27599, USA

ABSTRACT

The automatic capture of attention by drug cues, or attentional bias, is associated with craving and predicts future drug use. Despite its clinical significance, the neural bases of attentional bias to drug cues is not well understood. To address this gap, we undertook a neuroimaging investigation of the neural correlates of attentional bias towards smoking cues. Twenty-nine adults, including 14 active smokers and 15 non-smokers, completed a spatial cuing task during fMRI. A multivariate pattern analysis (MVPA) decoded the neural responses to the brief presentation of smoking versus neutral images. These data were correlated with behavioral measures of attentional bias, which included analyses targeting the neural correlates of response facilitation and cue-related task interference. We detected a set of brain-behavioral correlates that were similar across both smokers and non-smokers, indicating a role for stimuli salience in the absence of nicotine conditioning in smoking cue attentional bias. However, multiple smoking-related modifications to the neural correlates of attentional bias and its components were also identified. For example, regions demonstrating smoking-related differences in the neural correlates of attentional bias included the rostral anterior cingulate cortex and inferior frontal gyrus. Response facilitation effects of smoking were observed in the right orbitofrontal gyrus and bilateral middle temporal gyrus. Smoking-cue related task interference was related to smoking-related effects in the frontal eye fields. Our findings suggest that multiple cognitive, affective, and visual object recognition processes contribute to attentional bias towards smoking cues, and suggest multiple circuit modifications that may contribute to perpetuation of addiction.

1. Introduction

Craving for addictive substances can be readily elicited by exposure to drug-related cues. Evidence from laboratory-based tasks suggests that cue-triggered urges may result in part from abnormal allocation of attention to these drug-related stimuli, a process known as attentional bias (Field and Cox, 2008). Attentional bias predicts relapse risk (Cox et al., 2002; Cox et al., 2007; Marissen et al., 2006; Streeter et al., 2008; Waters et al., 2003), time to next drug use (Waters and Feyerabend, 2000), and quantity of drug use (Marhe et al., 2013); however, its ability to predict clinical outcomes might more precisely reflect its association with motivational states (Christiansen et al., 2015), as highlighted by strong evidence that the degree of bias associates with the extent of drug craving (Attwood et al., 2008; Field et al., 2005; Field et al., 2009; Franken et al., 2000; Mogg et al., 2003). As reduction of craving is a major focus of medication development for addictive

disorders (Waters et al., 2003), improving our understanding of its neural underpinnings is imperative.

In the laboratory, attentional bias towards drug cues is often indexed by variations in task performance associated with the presence of drug-related visual stimuli. Laboratory tasks designed to measure attentional bias to drug cues have included modified Stroop tasks utilizing drug-use words as stimuli (Ersche et al., 2010; Janes et al., 2010; Kilts et al., 2014), spatial cuing tasks (Chanon et al., 2010; Mogg et al., 2005; Wetherill et al., 2014), and change blindness paradigms (Jones et al., 2006; Jones et al., 2003). A spatial cuing task variant, the "dot-probe" task, consists of the brief presentation of image pairs, one drug use-related and one neutral, followed by a target (often a dot), appearing in the location previously occupied by either the drug cue or a neutral image. Studies indicate that when participants are instructed to respond quickly and accurately to the location of the target, individuals with substance use disorders generally respond more quickly to targets

appearing in the same spatial location in which a drug-related image had appeared, compared with targets appearing in place of a neutral image.

Several distinct processes are hypothesized to contribute to attentional bias among individuals with substance use disorders (Field and Cox, 2008; Mogg and Bradley, 2002; Mogg et al., 2005). Due to the relationship between craving and attentional bias during laboratory tasks, bias towards drug-related cues may stem from internal motivational states (Franken et al., 2000). Attentional bias to smoking-related images during a spatial cuing task also correlates with approach bias (Mogg et al., 2005), indicating possible overlapping mechanisms between these behaviors. Attentional bias among nicotine-dependent active smokers during a smoking word Stroop task was associated with increased activity in the insula, amygdala, hippocampus, parahippocampal gyrus, proposed to represent enhanced processing of internal states reflecting conditioned responses to drug cues (Janes et al., 2010). Neural activation of the right dorsal anterior cingulate cortex during fMRI in response to cocaine-related stimuli, which predicted future cocaine use among individuals with cocaine dependence, has been attributed to the enhanced cognitive control required to manage the conflict between task response requirements and automated processes elicited by drug-related words (Marhe et al., 2013). Enhanced activity in visual cortex in that study also indicated a role for enhanced sensory processing in attentional bias. In another study of individuals with cocaine dependence, attentional bias to drug-related words was positively correlated with activation of a network of regions involved in salience attribution and a frontal-temporal network that also related to processing of negative emotional stimuli; activity within a sensorimotor network predicted less attentional bias towards cocaine words (Kilts et al., 2014). Individuals with stimulant dependence also demonstrate activation of the left inferior frontal gyrus and right cerebellar cortex related to attentional bias during a drug-word Stroop task (Ersche et al., 2010). Thus, although findings remain inconsistent across drug-addicted populations and task designs, emphasizing the need for additional work in this area, the above studies suggest that multiple processes likely contribute to attentional bias. In the current study, we utilized a task designed to differentiate some of these processes. We hypothesized that several distinct processes contributing to attentional bias could be resolved by parsing out components of the attentional bias behavioral measure.

In this study, 14 active smokers (AS) and 15 non-smokers (NS) participated in a functional magnetic resonance imaging (fMRI) investigation of attentional bias to visual smoking cues, which used an fMRI dot-probe spatial cuing task to measure automatic attentional capture. We opted to use a task that included naturalistic images rather than words in order to engage neural processes of attentional bias related to visual object processing that are particularly relevant for real-world attentional bias. Importantly, we included a set of double neutral image trials to support our goal of distinguishing between components of attentional bias (Chanon et al., 2010; Cisler and Koster, 2010). Two distinct processes that may underlie behavioral measures of attentional bias include the facilitation of attentional capture by smoking cues on congruent trials and/or conflict between automatic attention towards smoking cues and task goals in incongruent trials. Thus, in addition to investigating the neural correlates of smoking attentional bias as typically defined in this task - the difference in reaction time (RT) between incongruent and congruent trials, we further considered congruent versus neutral trials (response facilitation) and incongruent versus neutral trials (smoking cue interference) to identify the neural correlates of these previously unexplored processes. To sensitively classify patterns of voxels representing smoking cue-induced brain activation, we applied a multivariate pattern analysis (MVPA) to the fMRI data (Haxby, 2012; Norman et al., 2006). Our findings suggest that neural processes contributing to smoking cue-related attentional bias involve a constellation of brain regions implicated in cognitive, affective, motor, and visual processes.

Table 1
Sample characteristics.

	Active smokers (mean ± SEM)	Non-smokers (mean ± sem)
N	14	15
Age (years)	24.8 ± 1.7	23.4 ± 0.9
Sex (males/females)	8/6	9/6
Race (white/black/other)	10/2/2	7/3/5
Cigarette dependence scale	42.6 ± 2.7	n/a
Time since last cigarette (min)	182.5 ± 83.4	n/a
Cigarettes/day	12 ± 1.7	n/a
Age smoking initiated (years)	17.6 ± 0.6	n/a
Years of cigarette use	7.1 ± 1.7	
Cigarette craving pre-scan	4.7 ± 0.6	n/a
Cigarette craving post-scan	7.1 ± 0.7	n/a
Barrett impulsiveness scale	70.1 ± 1.7	69.8 ± 1.1
State anxiety (STAI)	34.5 ± 2.6	31.5 ± 1.7
Trait Anxiety (STAI)	41.4 ± 3.1	35.5 ± 2.0
Thought-action fusion scale	16.4 ± 2.7	19.7 ± 2.7
Affect misattribution procedure: smoking-neutral ratings	−0.07 ± 0.05	−0.10 ± 0.03

2. Methods

2.1. Participants

Active smokers (AS; n = 14, 6 females) and non-smokers (NS; n = 15, 6 females), were recruited from the University of North Carolina at Chapel Hill (UNC) campus and surrounding community via informational e-mails and posted flyers. Prior to recruitment, participants completed an online or telephone-based questionnaire regarding their smoking habits. For inclusion in the AS group, participants needed to smoke at least 5 cigarettes per day on average (group average: 12.0 cigarettes/day, standard deviation: 6.3 range: 5–25). There were no instructions to abstain from smoking prior to the study session; the number of minutes since participants smoked their last cigarette was recorded and is summarized in Table 1. Occasional and former smokers were excluded from the non-smoking group. All subjects were between 18 and 40 years of age, right-handed, and were screened and excluded for neurological and psychiatric disease, current use of other psychoactive drugs, including medications, excepting moderate caffeine or alcohol intake, and contraindications to fMRI. Sample characteristics are summarized in Table 1.

2.2. Experimental task

After obtaining informed consent, participants completed a battery of self-administered, paper and pencil questionnaires including: The Cigarette Dependence Scale (CDS) (Etter et al., 2003), the Barratt Impulsiveness Scale (BIS) (Barratt and Stanford, 1995), the State-Trait Anxiety Inventory (STAI) (Spielberger et al., 1970), the Thought-Action Fusion Scale (TAF-scale) (Shafran et al., 1996), and a questionnaire developed in-house to assess smoking history, habits, and motivations. Additionally, a measurement of breath carbon monoxide levels was taken before beginning the task practice. At that time, participants also rated current cigarette craving on a scale of 1 (no craving) to 10 (most intense craving ever experienced). A second measure of craving was completed following the fMRI scan.

The spatial cuing task, implemented with *E*-Prime 1.2 (PST Inc., Pittsburgh, PA), was a variation of a dot-probe task, a type of behavioral task that has been used extensively to elicit attentional bias to drug-related stimuli (Chanon et al., 2010; Domaradzka and Bielecki, 2017; Ehrman et al., 2002; Wetherill et al., 2014), or to other types of salient stimuli (Lipp and Derakshan, 2005; MacLeod et al., 1986; Salemink et al., 2007). This particular version of the task has been previously described and validated in a behavioral study of attentional bias (Chanon et al., 2010). In that previous study, active smokers

demonstrated significantly greater attentional bias towards smoking images compared with non-smokers, providing good evidence for construct validity for this task variant. An additional experiment further demonstrated that reaction time effects produced by smoking images in this task are not likely driven simply by smokers' familiarity with the stimuli (Chanon et al., 2010). In each trial of the task, two grayscale images (11.1° × 9.0°) appeared, one on each side of a fixation cross. Importantly, we selected a task that included images rather than words, as these more naturalistic stimuli were intended to engage neural processes of attentional bias related to visual object processing that are particularly relevant for real-world attentional bias. The pairs of pictures consisted of either two neutral images or one smoking and one neutral image. The task design included trials with two neutral images not only to provide a requisite neuroimaging contrast, but also to differentiate the distinct processes that contribute to behavioral indices of attentional bias (Chanon et al., 2010; Cisler and Koster, 2010). Each image pair was presented for 150 ms. Smoking images were randomly presented on the left or right side of the screen and appeared an equal number of times on each side. Following a 50 ms inter-stimulus interval, both images disappeared and were replaced by either one dot (non-target) or two dots (target) for 100 ms. One-third of all trials consisted of "catch trials," in which the images were not followed by any targets, an fMRI task design strategy intended to enable statistical separation of the neural signals related to image presentation and target responding. The stimulus sets were matched in terms of the presence of people and hands and were also analyzed with respect to their spatial frequency content to ensure that they did not differ in terms of basic visual properties. On measures of both the spectral peak (Neutral: 0.020, Smoking: 0.021, $t = -0.07$, $p = 0.95$), and spectral width (Neutral: 54.81, Smoking: 54.01, $t = 0.18$, $p = 0.86$), the two stimulus sets did not differ. Subjects practiced one block of the cuing task in a mock scanner prior to the actual scan.

Following the practice and prior to entering the fMRI scanner, participants completed a block of the Affect Misattribution Procedure, which measures implicit affective responses to visual cues (Payne et al., 2007). In this task, implemented using *E*-Prime, participants saw an image (either smoking or neutral) for 75 ms, immediately followed by a blank screen for 125 ms, then a Chinese pictograph for 100 ms, and finally a screen of white noise until the participant responded. Participants were instructed to ignore the image and respond with one button if they found the pictograph to be pleasant and another if they found it unpleasant. They were warned that the image appearing before the pictograph could influence their responses and were instructed to try to avoid that to the best of their ability.

Once in the MR scanner, participants completed 4 blocks of 120 trials each of the spatial cuing task (Fig. 1). Subjects were instructed to fix their gaze on the cross and to respond with a button press corresponding to the side of the target (two dots) using an MRI-compatible button box.

Subjects were compensated $20/h. The entire experiment, including training, completion of questionnaires, and the scanning session lasted approximately 2 h. The spatial-cuing task in the scanner lasted approximately 30 min, and an additional three blocks of an attentional blink task (not reported here) took an additional 30 min. All procedures were approved by the UNC Office of Human Research Ethics.

2.3. Analysis of behavioral data

Three trial types were defined: "neutral trials" included the presentation of side-by-side neutral images followed by a target appearing on either side; "congruent trials" included the side-by-side presentation of one smoking image and one neutral image followed by a target in the location previously occupied by the smoking image; "incongruent trials" included the side-by-side presentation of one smoking image and one neutral image followed by a target in the location previously occupied by the neutral image. The primary measure of attentional bias

was determined by RT differences between incongruent and congruent trials. We further subdivided the attentional bias measure into distinct components. To isolate two potential mechanisms of attentional bias – facilitation of attentional capture by smoking cues in congruent trials or distraction from task goals by the smoking cues in incongruent trials – we calculated the RT differences between neutral and congruent trials (neutral minus congruent) and between incongruent and neutral trials (incongruent minus neutral). Only RTs from correct trials and trials with reaction times > 200 ms were included in calculations.

The effects of smoking status and trial type on accuracy and RT were tested in two-way repeated-measures analyses of variance (ANOVA) with group (active smokers and non-smokers) and trial type (neutral, congruent, and incongruent) as factors using the SAS (SAS 9.4. Cary, NC: SAS Institute Inc.) MIXED procedure. A follow-up analysis was conducted to explore whether a greater severity of smoking would associate with an enhanced attentional bias behavioral effect. For that analysis, the ANOVA models were altered to only include nonsmokers and the subset of smokers reporting smoking at least 10 cigarettes per day (n = 8). A third set of ANOVAs included only smokers and tested factors of trial type, time since last cigarette, and their interaction on accuracy and RT.

2.4. Image acquisition

Structural and functional images were acquired on a Siemens Magnetom Allegra 3 T MR scanner. Echo-planar images were acquired during four runs of the spatial cuing task using the following parameters: TR = 2200 ms, TE = 30 ms, FA = 80°, voxel size = 3.5 × 3.5 × 3.5 mm³, FOV = 224 × 224 mm², 37 coronal slices. For registration and tissue segmentation purposes, a high resolution T1 structural image was acquired with an MPRAGE sequence using the following parameters: TR = 1750 ms, TE = 4.38 ms, FA = 8°, voxel size = 1.0 × 1.0 × 1.0 mm³, FOV = 256 × 208 mm², 160 axial slices. A low resolution structural image was acquired to aid in registration between the functional and high-resolution structural images: TR = 500 ms, TE = 9 ms, FA1 = 90°, FA2 = 150°, slice thickness = 3.5 mm, voxel size = 1.8 × 1.8 × 3.5 mm³, FOV = 224 × 224 mm², 37 coronal slices.

2.5. Image preprocessing

Prior to statistical analyses, functional images were slice timing corrected and realigned with Statistical Parametric Mapping 8 (SPM8). Time series were scaled to percent signal change using Analysis of Functional Neuroimages (AFNI (Cox, 1996), version 16.2.07). A gray matter mask was created for each subject using the FSL fast segmentation process applied to each subject's high resolution T1 image. Images remained in subject space and were not spatially smoothed prior to MVPA in order to preserve subject-specific patterns of activations.

2.6. Calculation of activation maps

The task was modeled in SPM with events modeled as delta functions and convolved with a canonical hemodynamic response function. Since the task included cue-only catch trials, we were able to model image presentation and targets separately; therefore, we modeled five different event types: two neutral images (neutral trial), one smoking and one neutral image, targets following neutral trials, targets congruent with smoking images, and targets incongruent with smoking images. Each of the four fMRI task runs was further divided into 3, 52-frame data sets, yielding 12 total datasets per subject. A general linear model implemented in AFNI (3dDeconvolve and 3dREMLfit) tested the relationship between each of the five conditions and the fMRI time series across the 52 frames. Several nuisance variables representing likely sources of noise in the fMRI data were also included as covariates in the model: 6 directions of head motion, first 5 principal components
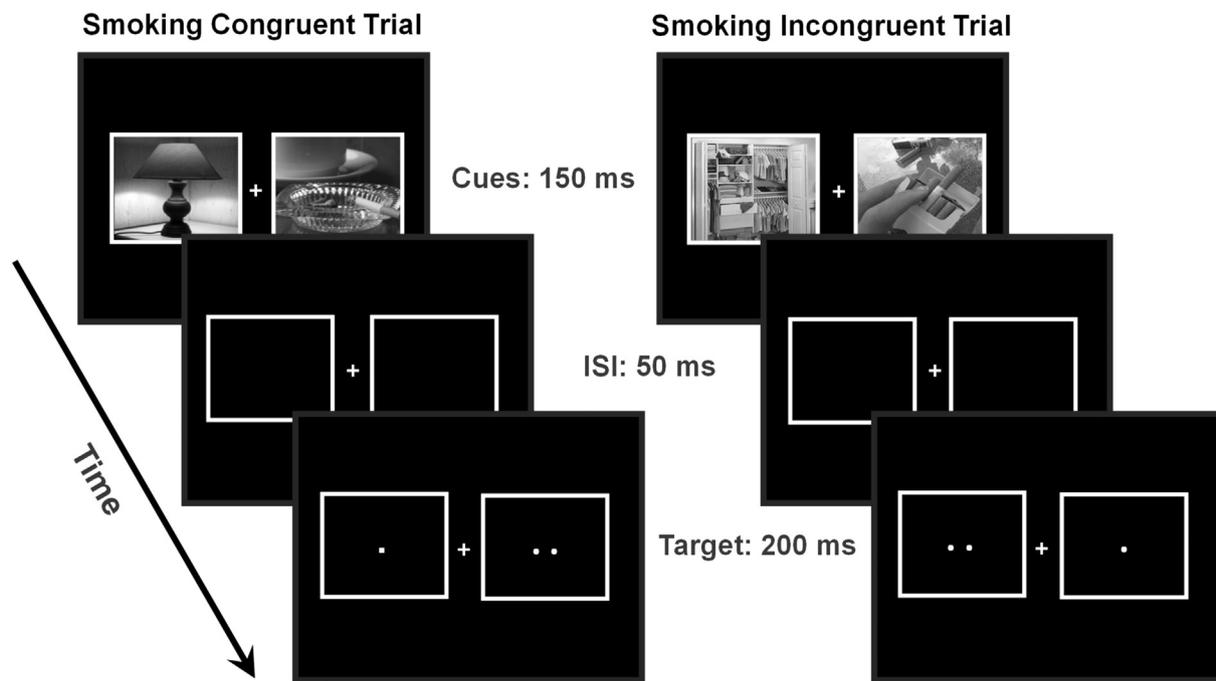
Smoking Congruent Trial   Smoking Incongruent Trial

Fig. 1. Spatial cuing task to measure attentional bias to smoking cues. Sample trial sequences are displayed for congruent trials (left), in which the target (i.e., two dots) appeared on the same side as the smoking-related image, and incongruent trials (right) in which the target appeared opposite of the smoking-related image. The task also included neutral trials in which both images were neutral images. ISI, inter-stimulus interval.

of signals from masks encompassing cerebrospinal fluid and white matter voxels, and first and second order trends. Beta maps of neuroactivation estimates when two neutral images were presented versus when a smoking image was presented were subsequently entered into multivariate pattern analyses.

2.7. Multivariate pattern analysis

In this analysis, we sought to identify sets of brain voxels that accurately distinguished between the presence versus absence of a smoking-related image. The presentation of a smoking image, relative to the presentation of two neutral images, contributes to RT differences in the response to a subsequent target (Chanon et al., 2010). Therefore, differences in patterns of neural responses between smoking and neutral conditions should theoretically account for variance in RT to the target (or "probe"). Advantages of focusing our analysis on neural responses to the presentation of smoking and neutral images – rather than the statistically-independent probes that follow – include the ability to better isolate the neural correlates of attentional capture by smoking cues and an improvement in power for the multivariate pattern analysis (probe types were divided into three categories versus only two categories of image presentation trials).

MVPA has emerged as an alternative method of examining brain activation during task fMRI as opposed to univariate tests which are performed on each voxel independently (Haxby, 2012; Norman et al., 2006). Multivariate pattern analysis of fMRI data was performed with the Princeton MVPA toolbox for Matlab in MATLAB13a. A spherical "searchlight" (Kriegeskorte et al., 2006) consisting of a center voxel and all its immediate neighbors (1 voxel radius) was passed across every voxel within each subject's gray matter mask. A Gaussian Naïve Bayes (GNB) binary classifier was created for sets of voxels within each searchlight location to classify patterns of voxel activation during trials containing smoking images versus those with two neutral images. A leave-one-out cross-validation procedure was applied across the 12 datasets to derive an unbiased measure of predictor accuracy. The center voxel of each searchlight was assigned the average cross-validation accuracy across the 12 datasets, resulting in a whole-brain map

of accuracy values for each subject.

2.8. Group-level statistical analysis and correction for multiple comparisons

Subject-level datasets were warped to MNI standard space in AFNI for group analysis using a nearest neighbor interpolation. To improve correspondence between subjects, which is limited by variation in functional anatomy, and to improve the signal-to-noise ratio of the accuracy data, we spatially smoothed accuracy maps using a 10 mm full-width at half maximum (FWHM) Gaussian kernel. We then calculated a group gray matter mask and applied it to all images. We detected brain regions showing statistically significant discrimination between conditions with a two step process: 1) Heteroscedastic linear models employed in FVGWAS software for MATLAB (Huang et al., 2015) tested the relationship between attentional bias behavioral measures and accuracy maps; this is a nonparametric analysis which makes no assumptions regarding data distributions. 2) A correction for multiple comparisons was employed to control family-wise error rates. In FCGWAS, two wild bootstrapping methods (Huang et al., 2015; Zhu et al., 2007) were used to generate null distributions of the maximum test statistic and maximum cluster size statistic (given $p < 0.005$), respectively. Voxels exceeding the 95th percentile maximum test statistic or clusters of voxels exceeding the 95th percentile maximum cluster size statistic were considered significant ($\alpha = 0.05$).

These group-level analyses tested two types of effects: 1) the effects of attentional bias on MVPA accuracy across all subjects and 2) the effects of the interaction of smoking group and attentional bias on MVPA accuracy. The first set of analyses examined the neural underpinnings of the visual detection of salient stimuli, a key process in the allocation of visual attention (Parkhurst et al., 2002) that has implications for attentional bias in addiction (Kilts et al., 2014; Marhe et al., 2013). The latter analysis was designed to isolate those elements of smoking-cue attentional bias specifically associated with nicotine conditioning among active smokers. All analyses controlled for age and sex.

Table 2
Spatial-cuing attentional bias task accuracy and reaction times by trial type.

	Overall (mean ± SEM)	Neutral (mean ± SEM)	Congruent (mean ± SEM)	Incongruent (mean ± SEM)
Accuracy				
Active smokers	0.92 ± 0.02	0.92 ± 0.03	0.92 ± 0.02	0.93 ± 0.02
Non-smokers	0.93 ± 0.02	0.93 ± 0.02	0.94 ± 0.02	0.94 ± 0.02
Average reaction time (ms)				
Active smokers	436.8 ± 6.8	437.6 ± 6.6	434.8 ± 7.3	438.1 ± 6.7
Non-smokers	449.1 ± 14.4	450.5 ± 14.6	447.6 ± 14.2	449.3 ± 14.4

3. Results

Smokers and non-smokers did not differ on any sample characteristic measures (Table 1), aside from their use of cigarettes. Smokers' scores on the Cigarette Dependence Scale (Table 1) were well within the norm of a random sample of adult smokers (Etter et al., 2003). Craving ratings among smokers were significantly higher after the fMRI scan than before, based on a paired samples *t*-test ($t = 3.59$, $p < 0.003$).

3.1. Behavioral

Participants completed the spatial cuing task with high levels of accuracy (see Table 2). A two-way repeated-measures analysis of variance indicated that average task accuracy did not differ between neutral, congruent, and incongruent trial types ($F(2,27) = 1.99$, $p = 0.16$; Table 2) or between active smoker and non-smoker groups ($F(1,27) = 0.14$, $p = 0.91$; Table 2), and there was no group-by-trial-type interaction ($F(2,27) = 0.79$, $p = 0.46$). However, there was a significant effect of trial type on RTs ($F(2,27) = 9.93$, $p < 0.001$; Table 2). RTs did not differ between the groups ($F(1,27) = 0.28$, $p = 0.60$; Table 2) and there was no group-by-trial-type interaction ($F(2,27) = 0.44$, $p = 0.65$).

Post-hoc tests of RT effects indicated that congruent trial RTs were significantly faster than incongruent trial RTs, indicating a significant attentional bias effect (whole sample: $t = -4.36$, $p < 0.001$), which was observed for both active smokers ($t = 2.36$, $p = 0.004$) and non-smokers ($t = 2.30$, $p = 0.037$). Congruent trial RTs were also significantly faster than neutral trial RTs (whole sample: $t = -3.05$, $p = 0.005$), but the response facilitation effect of congruent trials was only significant for active smokers (smokers: $t = 2.47$, $p = 0.028$; non-smokers $t = 1.52$, $p = 0.15$). However, neutral and incongruent trial RTs did not differ (whole sample: $t = 0.07$, $p = 0.94$; smokers: $t = -0.20$, $p = 0.84$; non-smokers $t = 0.15$, $p = 0.89$), suggesting that incongruent trials did not produce smoking cue interference. These effects are displayed in bar graphs for active smokers and non-smokers for each of the three RT contrasts in Fig. 2.

We also compared non-smokers to those smokers reporting smoking at least 10 cigarettes per day to explore whether the non-significant overall group differences in attentional bias may be related to the sample's relatively low levels of cigarette consumption (Fig. 2). Because this reduced the smoking sample to only 8 participants, we used a bootstrapping analysis (10,000 iterations) to statistically compare differences in group mean bias scores. The subsample of heavier smokers demonstrated significantly greater attentional bias (incongruent versus congruent RTs) compared with non-smokers (95% *CI*: 0.16–8.54; $p = 0.043$). There were no differences detected for response facilitation (95% *CI*: −7.30–8.87; $p = 0.51$) or cue interference (95% *CI*: −3.74–12.01; $p = 0.19$).

The final set of ANOVAs did not detect a main effect of time since last cigarette on either RT ($F(1,10) = 0.44$, $p = 0.52$) or accuracy ($F(1,10) = 0.49$, $p = 0.50$), and there was no interaction between time since last cigarette and trial type on either RT ($F(1,10) = 0.31$, $p = 0.74$) or accuracy ($F(2,10) = 2.35$, $p = 0.15$).
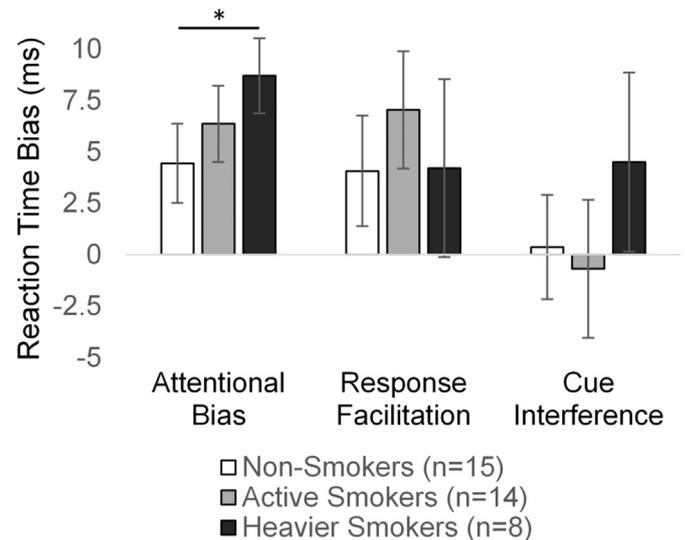

Fig. 2. Attentional bias to smoking cues: reaction time effects. Bar plots represent group means and standard errors of the means for reaction times related to attentional bias towards smoking cues (incongruent minus congruent trials), response facilitation (neutral minus congruent trials), and smoking cue interference (incongruent minus neutral trials).

Pearson's correlation analyses of the entire sample (n = 29) indicated that attentional bias towards smoking cues (incongruent RT minus congruent RT) was related to smoking cue interference (incongruent RT minus neutral RT) ($r = 0.40$, $p = 0.03$), but not to facilitation of responding to smoking-cue congruent targets (neutral RT minus congruent RT) ($r = 0.26$, $p = 0.17$). Interestingly, response facilitation effects and smoking cue interference effects were inversely correlated ($r = -0.78$, $p < 0.001$), suggesting that attentional bias effects may be more strongly related to response facilitation in some individuals and to smoking cue interference in others. Behavioral data by smoking group and trial type are presented in Table 2.

Pleasantness ratings for smoking versus neutral images during the Affect Misattribution Procedure were also not significantly correlated with attentional bias score ($r = -0.20$, $p = 0.31$), response facilitation ($r = -0.14$, $p = 0.48$), or smoking cue interference ($r = -0.00$, $p = 0.99$) based on Pearson's correlations. Changes in craving were not significantly related to attentional bias scores ($\rho = 0.32$, $p = 0.29$), response facilitation ($\rho = 0.32$, $p = 0.28$), or smoking cue interference ($\rho = -0.31$, $p = 0.29$) based on Spearman's correlations.

3.2. fMRI

The results of analyses of the MVPA neural correlates of attentional bias towards smoking cues are presented in Table 3.

3.2.1. Attentional bias towards smoking cues

As our primary measure of bias towards smoking cues, we calculated the difference in RT between incongruent and congruent trials.

Table 3
Multivariate pattern analysis correlates of smoking cue attentional bias.

Region	# Voxels	x	y	z
A. Attentional bias towards smoking cues				
Negative				
L posterior insula/precentral gyrus	6	−46	−4	9
L middle frontal gyrus	5	−46	25	34
	1	−24	47	18
	1	−38	34	18
R cerebellum	4	14	−51	−44
R anterior insula	2	29	21	1
	1	31	−3	5
L fusiform gyrus	2	−32	−50	−15
B. Attentional bias towards smoking cues interaction with group				
Positive				
R postcentral gyrus	1	55	−13	22
Negative				
L rostral anterior cingulate cortex	13	−8	45	−4
R rostral anterior cingulate cortex	2	14	45	8
L inferior frontal gyrus (pars triangularis)	2	−55	−19	10
L cerebellum	2	−16	−46	−43
C. Bias attributed to response facilitation				
Positive				
L cerebellum	10	−14	−56	−23
R superior parietal lobule	3	21	−45	64
Negative				
R insula	3	35	8	15
R inferior frontal gyrus (pars opercularis)	1	−34	−41	−17
D. Bias attributed to response facilitation interaction with group				
Positive				
L middle temporal gyrus	2	−48	−40	4
R middle temporal gyrus	1	58	9	−13
Mid-cingulate cortex	1	8	−26	43
Brainstem	1	11	−17	−28
Negative				
R orbital frontal gyrus	4	16	23	−15
E. Bias attributed to smoking cue interference				
Negative				
R postcentral gyrus	5	17	−35	67
R temporal pole	2	50	10	−19
L fusiform gyrus	2	−32	−38	−27
L middle frontal gyrus	1	−50	22	23
	1	−27	63	9
L middle temporal gyrus	1	−64	−43	−2
F. Bias attributed to smoking cue interference interaction with group				
Negative				
R frontal eye field	4	35	3	44
L frontal eye field	2	−41	4	52

We identified several brain regions in which accuracy was associated with decreased attentional bias across the full sample (Fig. 3A–B; Table 3A). More critically, we also detected regions in which the relationship between accuracy and attentional bias significantly interacted with group. Specifically, we observed a more positive relationship in active smokers versus non-smokers between attentional bias and classification accuracy in the postcentral sulcus, whereas more negative relationships were detected in the rostral anterior cingulate cortex, left inferior frontal gyrus, and left cerebellum (Fig. 3C–D; Table 3B).

3.2.2. Attentional bias attributed to response facilitation

To measure facilitation of responding to targets appearing congruent with smoking images, we calculated the difference in RT between congruent and neutral trials. Across, the full sample, we identified regions in which classification accuracy was related to facilitation of responding to smoking congruent targets (Fig. 4A–B; Table 3C). Of greater interest were differences in response facilitation-related accuracy detected between active smokers and non-smokers, which we found in the bilateral middle temporal gyrus, midcingulate cortex, brainstem, and right orbitofrontal gyrus (Fig. 4C–D; Table 3D).

3.2.3. Attentional bias attributed to smoking cue interference

As detailed above, attentional bias may also derive from difficulty in executing task goals in the presence of distracting smoking cues. Thus, we examined the smoking cue-related neural responses associated with incongruent versus neutral trial RTs. Among all subjects, smoking cue interference effects were directly of inversely related to activity in several regions (Fig. 5A–B; Table 3E). However, group differences in the association between smoking cue interference and differential activation to smoking cues were only observed in the bilateral frontal eye fields, where a more positive relationship was observed for smokers versus non-smokers (Fig. 5C-D; Table 3F).

4. Discussion

In this study, we identified the neural substrates of attentional bias to smoking-related cues using a multivariate analysis of fMRI data during a spatial cuing task. We explored several components of the attentional bias score, as well as the distinct neural correlates putatively related to nicotine conditioning among active smokers. The findings indicate that attentional bias in a laboratory spatial cuing task associates with differential patterns of activation in regions implicated in cognitive control, salience detection, reward processing, motor responding, and visual object recognition, which may contribute to response facilitation and cue interference components of attentional bias.

Among all subjects, regardless of nicotine use, greater attentional bias to smoking cues was associated with differential activation patterns in the left middle frontal gyrus, left posterior insula, right anterior insula, right cerebellum, and left fusiform gyrus. For each of the detected voxels and clusters, greater MVPA accuracy was associated with less attentional bias towards smoking cues. The left middle frontal gyrus and right anterior insula are regions involved in executive control (Vincent et al., 2008) and salience detection (Seeley et al., 2007), respectively, and may be involved in maintaining focus on relevant stimuli in the presence of distracting stimuli (Dosenbach et al., 2008), such as salient, but task-irrelevant, smoking cues. The posterior insula is implicated in the processing of visceral responses and representing internal motivational states (Gottfried et al., 2003). In the context of attentional bias, activation patterns in this region may relate to automatic visceral responses to smoking stimuli that function to facilitate or delay attentional shifts towards task-relevant stimuli. The left fusiform gyrus cluster was approximately at the location of the fusiform face area, which is selectively activated by faces compared with objects (Kanwisher et al., 1997). During the visual probe task, this process may contribute to the automatic diversion of subjects' gaze during those trials that included images of people smoking.

Comparing active smokers to non-smokers in an attentional bias-by-group interaction analysis revealed a set of neural correlates of smoking cue attentional bias that may result from conditioned associations. The largest region of significant smoking group-specific MVPA accuracy consisted of two clusters spanning the left and right rostral anterior cingulate cortex (rACC)/ventromedial prefrontal cortex (vmPFC), a finding consistent with other drug cue-related attentional bias studies (Goldstein et al., 2009; Goldstein et al., 2007; Kilts et al., 2014). The rACC/vmPFC region is part of a dopamine circuit with the nucleus accumbens and ventral tegmental area (Der-Avakian and Markou, 2012; Haber and Knutson, 2010) and responds to subjectively rewarding stimuli (Haber and Knutson, 2010; Pujara et al., 2016; Vassena et al., 2014). This region has also been associated with cognitive control in the presence of conflicting emotional stimuli (Egner et al., 2008; Etkin et al., 2006; Kompus et al., 2009), suggesting that its role in drug cue attentional bias may involve regulating conditioned responses to emotionally-salient drug cues (Goldstein et al., 2007).

We also investigated the neural correlates of smoking cue facilitation of responding. Across all subjects, variation in MVPA accuracy within the cerebellum, posterior parietal lobe, right insula, and right inferior frontal gyrus explained variance in responses to congruent
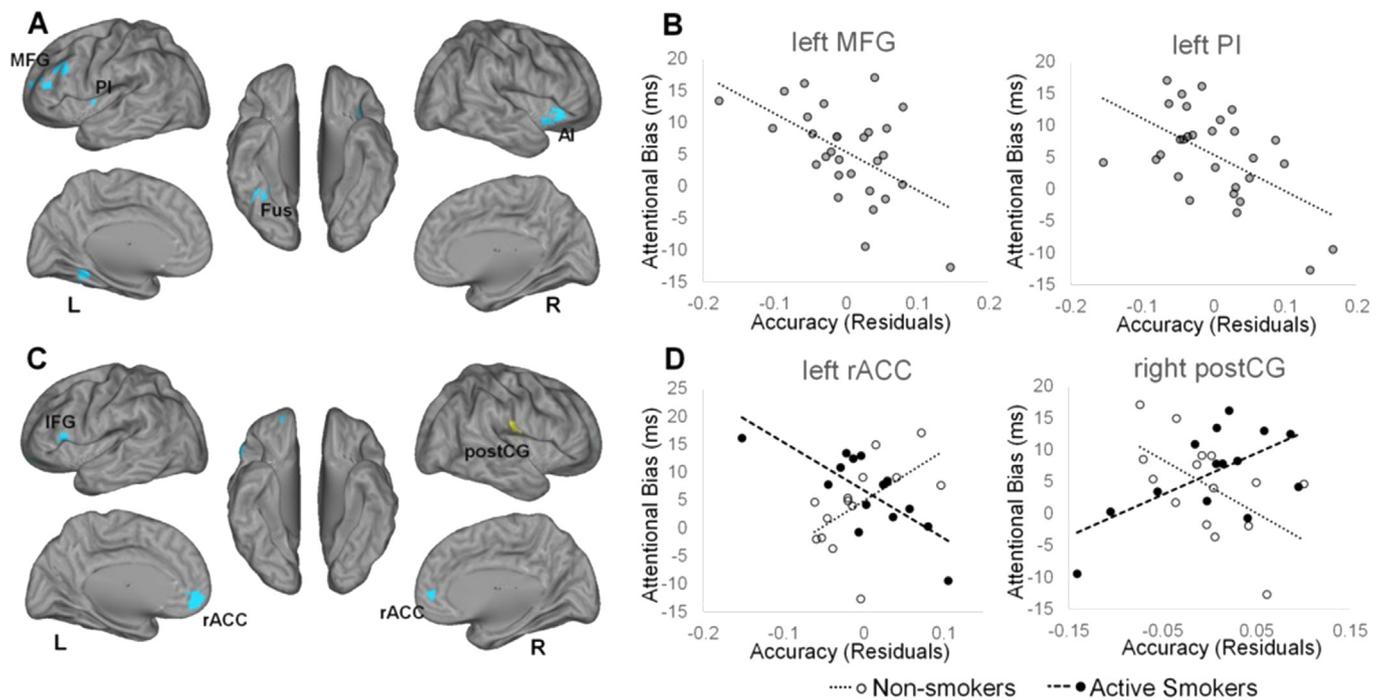
Fig. 3. Neural Correlates of attentional bias to smoking cues. Regions for which multivariate pattern analysis accuracy was significantly associated with reaction time differences between incongruent and congruent trials, A) for all subjects, B) including scatter plots for visualization of representative relationships, and C) for the interaction with smoking group, D) including scatter plots for visualization of representative relationships, are displayed on left and right cerebral hemispheres. Accuracy scores represent residuals of cluster-average accuracy, adjusting for participant age and sex, and are therefore centered on zero. Yellow color represents positive relationships. L, left; R, right; AI, anterior insula; Fus, fusiform gyrus; IFG, inferior frontal gyrus; MFG, middle frontal gyrus; PI, posterior insula; postCG, postcentral gyrus; rACC, rostral anterior cingulate cortex; postCG, postcentral gyrus. (For interpretation of the references to color in this figure legend, the reader is referred to the web version of this article.)
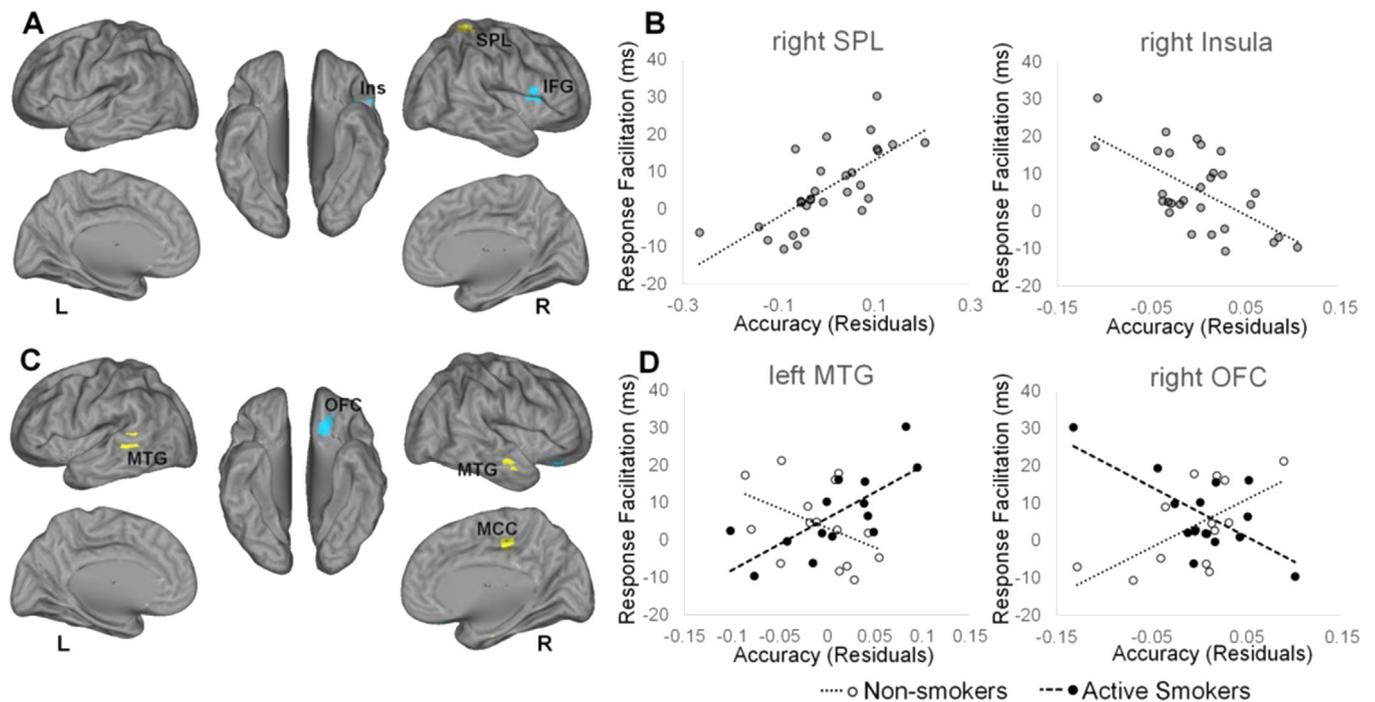

Fig. 4. Neural correlates of facilitated responding to smoking cues. Regions for which multivariate pattern analysis accuracy was significantly associated with reaction time differences between neutral and congruent trials, A) for all subjects, B) including scatter plots for visualization of representative relationships, and C) for the interaction with smoking group, D) including scatter plots for visualization of representative relationships, are displayed on left and right cerebral hemispheres. Accuracy scores represent residuals of cluster-average accuracy, adjusting for participant age and sex, and are therefore centered on zero. Yellow color represents positive relationships. Blue color represents negative relationships. L, left; R, right; IFG, inferior frontal gyrus; Ins, insula; MCC, mid-cingulate cortex; MTG, middle temporal gyrus; OFC, orbitofrontal cortex; SPL, superior parietal lobule. (For interpretation of the references to color in this figure legend, the reader is referred to the web version of this article.)
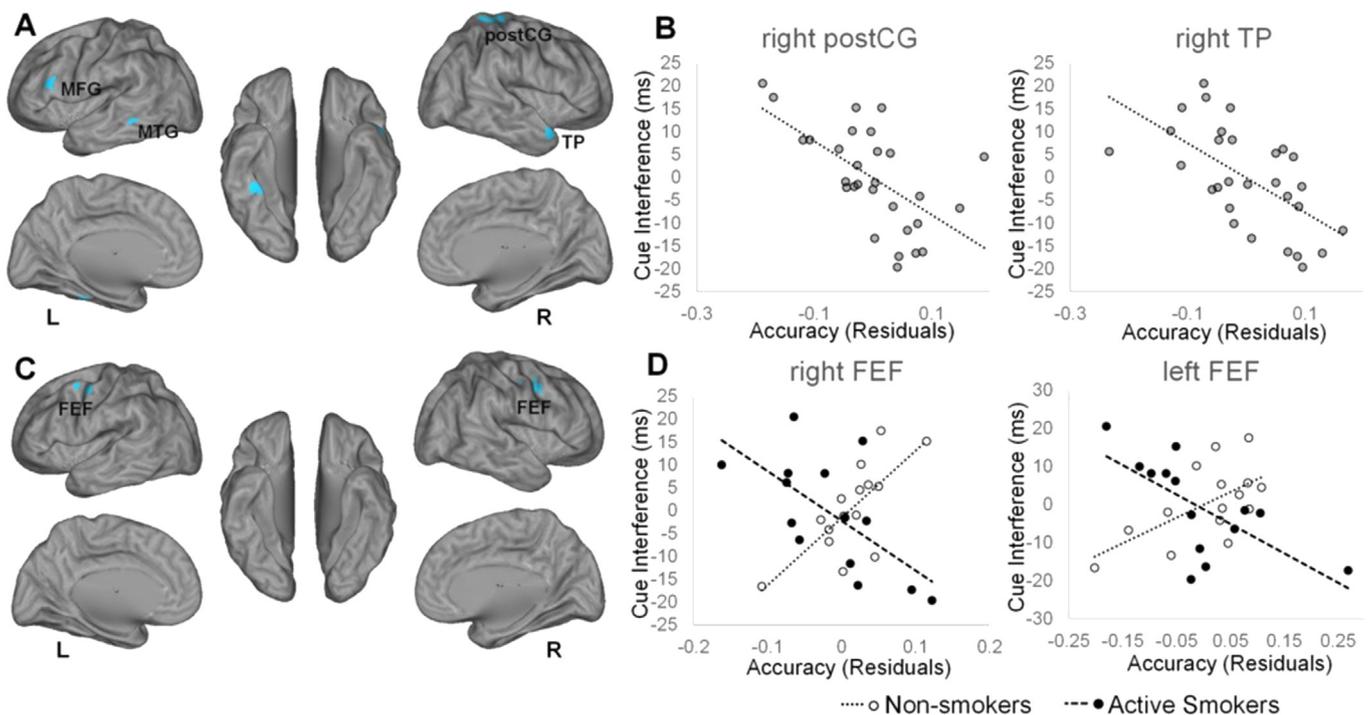
Fig. 5. Neural correlates of bias attributed to smoking cue interference. Regions for which multivariate pattern analysis accuracy was significantly associated with reaction time differences between incongruent and neutral trials, A) for all subjects, B) including scatter plots for visualization of representative relationships, and C) for the interaction with smoking group, D) including scatter plots for visualization of representative relationships, are displayed on left and right cerebral hemispheres. Accuracy scores represent residuals of cluster-average accuracy, adjusting for participant age and sex, and are therefore centered on zero. Yellow color represents positive relationships. Blue color represents negative relationships. L, left; R, right; MFG, middle frontal gyrus; MTG, middle temporal gyrus; postCG, postcentral gyrus; TP, temporal pole; FEF, frontal eye field. (For interpretation of the references to color in this figure legend, the reader is referred to the web version of this article.)

trials compared with neutral trials. The identified cerebellar cluster is highly correlated with the primary motor cortex and associated with motor execution (neurosynth.org, (Manto et al., 2012)), consistent with its association with the response facilitation component of attentional bias in the current study. The insula's association with attentional bias to smoking cues has been previously attributed to its role in processing emotionally-salient stimuli (Janes et al., 2010). Although response facilitation by smoking cues did not significantly correlate with our primary measure of attentional bias, the fact that we detected significant response facilitation only in smokers (Fig. 2), and that response facilitation was associated with a distinct set of neural correlates, suggests that variations in response facilitation processes may represent a functionally meaningful source of attentional bias for a subset of smokers. This assertion is further supported by our finding that response facilitation negatively correlated with smoking cue interference, indicating that these two mechanisms likely contribute independently to attentional bias to smoking cues. Differences between smokers and non-smokers in the neural correlates of response facilitation were observed in the bilateral middle temporal gyrus, mid-cingulate cortex, and brainstem (smokers > non-smokers), and in the right OFC (non-smokers > smokers). The lateral OFC is often engaged when responses for rewards require suppression of other reward-related cues (Elliott et al., 2000; Rogers et al., 1999), suggesting a potential role in facilitating responding among smokers, for whom smoking cues have acquired incentive salience. However, this region is also important for the fast recognition of visual stimuli (Bar et al., 2006; Kveraga et al., 2007), and may also integrate past affective experiences with current perceptions (Barrett and Bar, 2009); thus, the OFC may be differentially engaged among active smokers due to their more extensive familiarity and experience with smoking-related stimuli.

The neural correlates of attentional bias attributed to smoking cue interference across all subjects, quantified as RT differences between

incongruent and neutral trials, included clusters in the postcentral gyrus, temporal pole, left fusiform gyrus, middle frontal gyrus, and middle temporal gyrus. Consistent with the positive correlations between the primary measure of attentional bias and smoking cue interference, there were some similarities in the fMRI analysis of these two behavioral measures, particularly in the middle frontal gyrus and fusiform gyrus. Thus, these regions, and perhaps their inferred roles in executive control and visual facial processing, respectively, may contribute to a mechanism of attentional bias related to engaging cognitive control over the automatic capture of attention by smoking cues. Group differences in smoking cue interference effects were present in the frontal eye fields, a region involved in saccadic eye movements and visual attention. In particular, the relationship was positive in non-smokers and negative in smokers, indicating a possible nicotine conditioning effect on visual attention systems.

The attentional bias effect based on reaction times was non-significantly larger in active smokers versus non-smokers. However, we observed faster responding to congruent versus incongruent trials in both the smokers and non-smokers. The finding of significant smoking-cue attentional bias even among non-smokers is consistent with several prior studies (e.g., (Chanon et al., 2010; Ehrman et al., 2002; Forestell et al., 2012)) and suggests that conditioned responses to smoking images can be acquired in the absence of personal nicotine use. In this sample, only heavier smokers (at least 10 cigarettes per day) demonstrated significantly greater attentional bias scores than non-smokers. It is possible that a more severe clinical sample or a larger sample size would have yielded more significant group differences in attentional bias. Nonetheless, the current study as well as many others that have reported small or absent group behavioral differences (i.e., (Goldstein et al., 2009; Goldstein et al., 2010; Luijten et al., 2012; Luijten et al., 2011; Nestor et al., 2011) detected neuroimaging group differences that indicate smoking-related effects on the neural correlates of attentional

bias, possibly since similar behaviors may emerge from different neural mechanisms. Indeed, neuroimaging analyses enabled us to disentangle effects that are purely related to stimuli salience (whole group correlation), which are also observed in nonclinical samples, from conditioned drug effects or maladaptive neural processes among active smokers (interaction effects). Thus, the inclusion of a non-smoking sample represents a particular strength of the current study.

Several limitations of this study also deserve consideration. First, although we maximized our power by using correlational analyses, the study sample size is relatively small, raising concerns about undetected effects (Type II error), as well as the need for replication. Secondly, laboratory tasks likely provide imprecise correspondence to attentional bias in a real-world setting. For example, primary motor cortical activations may represent a task-specific finding relevant for manual button responses but not for real world drug-seeking behavior. Further efforts to include naturalistic imagery during fMRI sessions, as well as the evaluation of correspondence between attentional bias neuroactivation measures and drug use outcomes, are warranted. Additionally, although we attempted to interpret the roles of detected brain regions based on the known demands of the attentional bias task and the existing attentional bias literature, we cannot make conclusive inferences for these brain-behavior associations. Finally, we did not acquire eye tracking data during this study, which may have provided additional insight for interpreting the results.

5. Conclusions

We applied a multivariate approach to detecting the neural correlates of attentional bias to smoking cues. We report novel findings of the components of the neural response to smoking cues related to overall attentional bias, response facilitation, and smoking cue response interference. This study extends our knowledge of attentional processing in cigarette smokers by identifying a brain basis for behavioral responses to smoking-related images.

Acknowledgements

Funding

References

Attwood, A.S., O'Sullivan, H., Leonards, U., Mackintosh, B., Munafó, M.R., 2008. Attentional bias training and cue reactivity in cigarette smokers. Addiction 103 (11), 1875–1882.

Bar, M., Kassam, K.S., Ghuman, A.S., Boshyan, J., Schmid, A.M., Dale, A.M., Hamalainen, M.S., Marinkovic, K., Schacter, D.L., Rosen, B.R., Halgren, E., 2006. Top-down facilitation of visual recognition. Proc. Natl. Acad. Sci. U. S. A. 103 (2), 449–454.

Barratt, E.S., Stanford, M.S., 1995. Impulsiveness. In: Costello, C.G. (Ed.), Personality Characteristics of the Personality Disordered Client. Wiley, New York, pp. 91–118.

Barrett, L., Bar, M., 2009. See it with feeling: affective predictions during object perception. Philos. Trans. R. Soc. Lond. Ser. B Biol. Sci. 364 (1521), 1325–1334.

Chanon, V.W., Sours, C.R., Boettiger, C.A., 2010. Attentional bias toward cigarette cues in active smokers. Psychopharmacology 212 (3), 309–320.

Christiansen, P., Schoenmakers, T.M., Field, M., 2015. Less than meets the eye: reappraising the clinical relevance of attentional bias in addiction. Addict. Behav. 44, 43–50.

Cisler, J.M., Koster, E.H.W., 2010. Mechanisms of attentional biases towards threat in the anxiety disorders: an integrative review. Clin. Psychol. Rev. 30 (2), 203.

Cox, R.W., 1996. AFNI: software for analysis and visualization of functional magnetic resonance neuroimages. Comput. Biomed. Res. 29 (3), 162–173.

Cox, W.M., Hogan, L.M., Kristian, M.R., Race, J.H., 2002. Alcohol attentional bias as a predictor of alcohol abusers' treatment outcome. Drug Alcohol Depend. 68 (3), 237–243.

Cox, W.M., Pothos, E.M., Hosier, S.G., 2007. Cognitive-motivational predictors of excessive drinkers' success in changing. Psychopharmacology 192 (4), 499–510.

Der-Avakian, A., Markou, A., 2012. The neurobiology of anhedonia and other reward-related deficits. Trends Neurosci. 35 (1), 68–77.

Domaradzka, E., Bielecki, M., 2017. Deadly attraction – attentional bias toward preferred cigarette brand in smokers. Front. Psychol. 8.

Dosenbach, N.U.F., Fair, D.A., Cohen, A.L., Schlaggar, B.L., Petersen, S.E., 2008. A dual-networks architecture of top-down control. Trends Cogn. Sci. 12 (3), 99–105.

Egner, T., Etkin, A., Gale, S., Hirsch, J., 2008. Dissociable neural systems resolve conflict from emotional versus nonemotional distracters. Cereb. Cortex 18 (6), 1475–1484.

Ehrman, R.N., Robbins, S.J., Bromwell, M.A., Lankford, M.E., Monterosso, J.R., O'Brien, C.P., 2002. Comparing attentional bias to smoking cues in current smokers, former smokers, and non-smokers using a dot-probe task. Drug Alcohol Depend. 67 (2), 185–191.

Elliott, R., Dolan, R.J., Frith, C.D., 2000. Dissociable functions in the medial and lateral orbitofrontal cortex: evidence from human neuroimaging studies. Cereb. Cortex 10 (3), 308–317.

Ersche, K.D., Bullmore, E.T., Craig, K.J., Shabbir, S.S., Abbott, S., Muller, U., Ooi, C., Suckling, J., Barnes, A., Sahakian, B.J., Merlo-Pich, E.V., Robbins, T.W., 2010. Influence of compulsivity of drug abuse on dopaminergic modulation of attentional bias in stimulant dependence. Arch. Gen. Psychiatry 67 (6), 632–644.

Etkin, A., Egner, T., Peraza, D.M., Kandel, E.R., Hirsch, J., 2006. Resolving emotional conflict: a role for the rostral anterior cingulate cortex in modulating activity in the amygdala. Neuron 51 (6), 871–882.

Etter, J.F., Le Houezec, J., Perneger, T.V., 2003. A self-administered questionnaire to measure dependence on cigarettes: the cigarette dependence scale. Neuropsychopharmacology 28 (2), 359–370.

Field, M., Cox, W.M., 2008. Attentional bias in addictive behaviors: a review of its development, causes, and consequences. Drug Alcohol Depend. 97 (1–2), 1–20.

Field, M., Mogg, K., Bradley, B.P., 2005. Craving and cognitive biases for alcohol cues in social drinkers. Alcohol Alcohol. 40 (6), 504–510.

Field, M., Munafó, M.R., Franken, I.H., 2009. A meta-analytic investigation of the relationship between attentional bias and subjective craving in substance abuse. Psychol. Bull. 135 (4), 589–607.

Forestell, C.A., Dickter, C.L., Wright, J.D., Young, C.M., 2012. Clearing the smoke: parental influences on non-smokers' attentional biases to smoking-related cues. Psychol. Addict. Behav. 26 (3), 638–643.

Franken, I.H., Kroon, L.Y., Wiers, R.W., Jansen, A., 2000. Selective cognitive processing of drug cues in heroin dependence. J. Psychopharmacol. 14 (4), 395–400 (Oxford, England).

Goldstein, R.Z., Tomasi, D., Rajaram, S., Cottone, L.A., Zhang, L., Maloney, T., Telang, F., Alia-Klein, N., Volkow, N.D., 2007. Role of the anterior cingulate and medial orbitofrontal cortex in processing drug cues in cocaine addiction. Neuroscience 144 (4), 1153–1159.

Goldstein, R.Z., Alia-Klein, N., Tomasi, D., Carrillo, J.H., Maloney, T., Woicik, P.A., Wang, R., Telang, F., Volkow, N.D., 2009. Anterior cingulate cortex hypoactivations to an emotionally salient task in cocaine addiction. Proc. Natl. Acad. Sci. U. S. A. 106 (23), 9453–9458.

Goldstein, R.Z., Woicik, P.A., Maloney, T., Tomasi, D., Alia-Klein, N., Shan, J., Honorio, J., Samaras, D., Wang, R., Telang, F., Wang, G.J., Volkow, N.D., 2010. Oral methylphenidate normalizes cingulate activity in cocaine addiction during a salient cognitive task. Proc. Natl. Acad. Sci. U. S. A. 107 (38), 16667–16672.

Gottfried, J.A., O'Doherty, J., Dolan, R.J., 2003. Encoding predictive reward value in human amygdala and orbitofrontal cortex. Science 301 (5636), 1104–1107.

Haber, S.N., Knutson, B., 2010. The reward circuit: linking primate anatomy and human imaging. Neuropsychopharmacology 35 (1), 4–26.

Haxby, J.V., 2012. Multivariate pattern analysis of fMRI: the early beginnings. Neuroimage 62 (2), 852–855.

Huang, M., Nichols, T., Huang, C., Yu, Y., Lu, Z., Knickmeyer, R.C., Feng, Q., Zhu, H., 2015. FVGWAS: fast voxelwise genome wide association analysis of large-scale imaging genetic data. Neuroimage 118, 613–627.

Janes, A.C., Pizzagalli, D.A., Richardt, S., Frederick Bde, B., Holmes, A.J., Sousa, J., Fava, M., Evins, A.E., Kaufman, M.J., 2010. Neural substrates of attentional bias for smoking-related cues: an FMRI study. Neuropsychopharmacology 35 (12), 2339–2345.

Jones, B.T., Jones, B.C., Smith, H., Copley, N., 2003. A flicker paradigm for inducing change blindness reveals alcohol and cannabis information processing biases in social users. Addiction 98 (2), 235–244.

Jones, B.T., Bruce, G., Livingstone, S., Reed, E., 2006. Alcohol-related attentional bias in problem drinkers with the flicker change blindness paradigm. Psychol. Addict. Behav. 20 (2), 171–177.

Kanwisher, N., McDermott, J., Chun, M.M., 1997. The fusiform face area: a module in human extrastriate cortex specialized for face perception. J. Neurosci. 17 (11), 4302–4311.

Kilts, C.D., Kennedy, A., Elton, A.L., Tripathi, S.P., Young, J., Cisler, J.M., James, G.A., 2014. Individual differences in attentional bias associated with cocaine dependence are related to varying engagement of neural processing networks. Neuropsychopharmacology 39 (5), 1135–1147.

Kompus, K., Hugdahl, K., Ohman, A., Marklund, P., Nyberg, L., 2009. Distinct control networks for cognition and emotion in the prefrontal cortex. Neurosci. Lett. 467 (2), 76–80.

Kriegeskorte, N., Goebel, R., Bandettini, P., 2006. Information-based functional brain mapping. Proc. Natl. Acad. Sci. U. S. A. 103 (10), 3863–3868.

Kveraga, K., Boshyan, J., Bar, M., 2007. Magnocellular projections as the trigger of top-down facilitation in recognition. J. Neurosci. 27 (48), 13232–13240.

Lipp, O.V., Derakshan, N., 2005. Attentional bias to pictures of fear-relevant animals in a

dot probe task. Emotion 5 (3), 365–369.

Luijten, M., Veltman, D.J., van den Brink, W., Hester, R., Field, M., Smits, M., Franken, I.H., 2011. Neurobiological substrate of smoking-related attentional bias. Neuroimage 54 (3), 2374–2381.

Luijten, M., Veltman, D.J., Hester, R., Smits, M., Pepplinkhuizen, L., Franken, I.H.A., 2012. Brain activation associated with attentional bias in smokers is modulated by a dopamine antagonist. Neuropsychopharmacology 37 (13), 2772–2779.

MacLeod, C., Mathews, A., Tata, P., 1986. Attentional bias in emotional disorders. J. Abnorm. Psychol. 95 (1), 15–20.

Manto, M., Bower, J.M., Conforto, A.B., Delgado-García, J.M., da Guarda, S.N.F., Gerwig, M., Habas, C., Hagura, N., Ivry, R.B., Mariën, P., Molinari, M., Naito, E., Nowak, D.A., Ben Taib, N.O., Pelisson, D., Tesche, C.D., Tilikete, C., Timmann, D., 2012. Consensus paper: roles of the cerebellum in motor control—the diversity of ideas on cerebellar involvement in movement. Cerebellum 11 (2), 457–487.

Marhe, R., Luijten, M., van de Wetering, B.J.M., Smits, M., Franken, I.H.A., 2013. Individual differences in anterior cingulate activation associated with attentional Bias predict cocaine use after treatment. Neuropsychopharmacology 38 (6), 1085–1093.

Marissen, M.A., Franken, I.H., Waters, A.J., Blanken, P., van den Brink, W., Hendriks, V.M., 2006. Attentional bias predicts heroin relapse following treatment. Addiction 101 (9), 1306–1312.

Mogg, K., Bradley, B.P., 2002. Selective processing of smoking-related cues in smokers: manipulation of deprivation level and comparison of three measures of processing bias. J. Psychopharmacol. 16 (4), 385–392.

Mogg, K., Bradley, B.P., Field, M., De Houwer, J., 2003. Eye movements to smoking-related pictures in smokers: relationship between attentional biases and implicit and explicit measures of stimulus valence. Addiction 98 (6), 825–836.

Mogg, K., Field, M., Bradley, B.P., 2005. Attentional and approach biases for smoking cues in smokers: an investigation of competing theoretical views of addiction. Psychopharmacology 180 (2), 333–341.

Nestor, L., McCabe, E., Jones, J., Clancy, L., Garavan, H., 2011. Differences in "bottom-up" and "top-down" neural activity in current and former cigarette smokers: evidence for neural substrates which may promote nicotine abstinence through increased cognitive control. Neuroimage 56 (4), 2258–2275.

Norman, K.A., Polyn, S.M., Detre, G.J., Haxby, J.V., 2006. Beyond mind-reading: multi-voxel pattern analysis of fMRI data. Trends Cogn. Sci. 10 (9), 424–430.

Parkhurst, D., Law, K., Niebur, E., 2002. Modeling the role of salience in the allocation of overt visual attention. Vis. Res. 42 (1), 107–123.

Payne, B.K., McClernon, F.J., Dobbins, I.G., 2007. Automatic affective responses to smoking cues. Exp. Clin. Psychopharmacol. 15 (4), 400–409.

Pujara, M.S., Philippi, C.L., Motzkin, J.C., Baskaya, M.K., Koenigs, M., 2016. Ventromedial prefrontal cortex damage is associated with decreased ventral striatum volume and response to reward. J. Neurosci. 36 (18), 5047–5054.

Rogers, R.D., Owen, A.M., Middleton, H.C., Williams, E.J., Pickard, J.D., Sahakian, B.J., Robbins, T.W., 1999. Choosing between small, likely rewards and large, unlikely rewards activates inferior and orbital prefrontal cortex. J. Neurosci. 19 (20), 9029–9038.

Salemink, E., van den Hout, M.A., Kindt, M., 2007. Selective attention and threat: quick orienting versus slow disengagement and two versions of the dot probe task. Behav. Res. Ther. 45 (3), 607–615.

Seeley, W.W., Menon, V., Schatzberg, A.F., Keller, J., Glover, G.H., Kenna, H., Reiss, A.L., Greicius, M.D., 2007. Dissociable intrinsic connectivity networks for salience processing and executive control. J. Neurosci. 27 (9), 2349–2356.

Shafran, R., Thordarson, D.S., Rachman, S., 1996. Thought-action fusion in obsessive compulsive disorder. J. Anxiety Disord. 10 (5), 379–391.

Spielberger, C.D., Gorsuch, R.R., Luchene, R.E., 1970. State-Trait Anxiety Inventory. Consulting Psychologists Press, Palo Alto, CA.

Streeter, C.C., Terhune, D.B., Whitfield, T.H., Gruber, S., Sarid-Segal, O., Silveri, M.M., Tzilos, G., Afshar, M., Rouse, E.D., Tian, H., Renshaw, P.F., Ciraulo, D.A., Yurgelun-Todd, D.A., 2008. Performance on the Stroop predicts treatment compliance in cocaine-dependent individuals. Neuropsychopharmacology 33 (4), 827–836.

Vassena, E., Krebs, R.M., Silvetti, M., Fias, W., Verguts, T., 2014. Dissociating contributions of ACC and vmPFC in reward prediction, outcome, and choice. Neuropsychologia 59, 112–123.

Vincent, J.L., Kahn, I., Snyder, A.Z., Raichle, M.E., Buckner, R.L., 2008. Evidence for a frontoparietal control system revealed by intrinsic functional connectivity. J. Neurophysiol. 100 (6), 3328–3342.

Waters, A.J., Feyerabend, C., 2000. Determinants and effects of attentional bias in smokers. Psychol. Addict. Behav. 14 (2), 111–120.

Waters, A.J., Shiffman, S., Sayette, M.A., Paty, J.A., Gwaltney, C.J., Balabanis, M.H., 2003. Attentional bias predicts outcome in smoking cessation. Health Psychol. 22 (4), 378–387.

Wetherill, R.R., Jagannathan, K., Lohoff, F.W., Ehrman, R., O'Brien, C.P., Childress, A.R., Franklin, T.R., 2014. Neural correlates of attentional bias for smoking cues: modulation by variance in the dopamine transporter gene. Addict. Biol. 19 (2), 294–304.

Zhu, H., Ibrahim, J.G., Tang, N., Rowe, D.B., Hao, X., Bansal, R., Peterson, B.S., 2007. A statistical analysis of brain morphology using wild bootstrapping. IEEE Trans. Med. Imaging 26 (7), 954–966.